



1 **Big data managing in a landslide Early Warning System: experience from a ground-based**
2 **interferometric radar application**

3 Emanuele Intriери¹, Federica Bardi¹, Riccardo Fanti¹, Giovanni Gigli¹, Francesco Fidolini², Nicola
4 Casagli¹, Sandra Costanzo³, Antonio Raffo³, Giuseppe Di Massa³, Giovanna Capparelli³, Pasquale
5 Versace³.

6 ¹Department of Earth Sciences, University of Florence, via La Pira 4, 50121, Florence, Italy

7 ²Pizzi Terra srl, via di Ripoli 207H, 50126, Florence, Italy

8 ³Department of Soil Defense, University of Calabria, Ponte Pietro Bucci, Cube 41b, 87036,
9 Arcavacata di Rende (CS), Italy

10

11 *Correspondence to:* Emanuele Intriери (emanuele.intriери@unifi.it)

12

13

14 **Keywords:** early warning system; slope instability; big data; monitoring; landslide; risk
15 management; ground-based interferometric radar

16

17 **1 Abstract**

18 A big challenge in terms of landslide risk mitigation is represented by the increasing of the
19 resiliency of society exposed to the risk. Among the possible strategies to reach this goal, there is
20 the implementation of early warning systems. This paper describes a procedure to improve early
21 warning activities in areas affected by high landslide risk, such as those classified as Critical
22 Infrastructures for their central role in society.

23 This research is part of the project “LEWIS (Landslides Early Warning Integrated System): An
24 Integrated System for Landslide Monitoring, Early Warning and Risk Mitigation along Lifelines”.

25 LEWIS is composed of a susceptibility assessment methodology providing information for single
26 points and areal monitoring systems, a data transmission network and a Data Collecting And
27 Processing Center (DCPC), where readings from all monitoring systems and mathematical models
28 converge and which sets the basis for warning and intervention activities.

29 In this paper we will focus on the interaction between an areal monitoring tool (a ground-based
30 interferometric radar) and the DCPC, and how issues such as big data transfer, real-time warning,
31 line of sight correction and data validation in emergency conditions have been dealt with.

32

33 **2 Introduction**

34 Urbanization, especially in mountain areas, can be considered a major cause for high landslide risk
35 because of the increased exposure of elements at risk. Among the elements at risk, important
36 communication routes, such as highways, can be classified as Critical Infrastructures (CIs), since
37 their rupture can cause chain effects with catastrophic damages on society (Geertsema et al 2009;
38 Kadri et al. 2014). On the other hand, modern society is more and more dependent from CIs and



39 their continuous efficiency (Lebaka et al., 2016), and this has risen their value over the years. The
40 result is a higher social vulnerability in the face of loss of continuous operation (Kröger, 2008). The
41 main objective was to improve the social preparedness to the growing landslide risk, according with
42 the suggestions of several authors (Gene Corley et al., 1998; Baldrige et al., 2011; Urlainis et al.
43 2014; 2015). This led to the development of several approaches and frameworks for increasing the
44 resiliency of society exposed to the risk (Kröger, 2008; Cagno et al., 2011 and references therein).
45 The resiliency policy of course involves prevention activities but also, and more importantly, those
46 activities needed to maintain functionality after disruption (Snyder and Burns, 2009) and to
47 promptly alert incoming catastrophes in order to protect people and prepare for a possible damaging
48 of the endangered CI. Among these activities, the implementation of integrated landslides early
49 warning systems (*i.e.* LEWIS, Versace et al., 2012; Costanzo et al., 2016) reveals its increasing
50 importance.

51 In this context, the methodology described in this paper has been conceived; it has been tested and
52 validated on a portion of an Italian highway, affected by landslides and selected as case study: it is
53 located in Southern Italy, along a section of the A16 highway, an important communication route
54 that connects Naples to Bari.

55 A ground based interferometer (GB-InSAR) has been installed on the test site, in order to obtain
56 aerial monitoring data. The installation was in an area where the only internet connection available
57 was 3G, with a limit of 2 gigabyte data transfer per month. Nevertheless, these data could be
58 managed thanks to the implemented data transmission network and Data Collecting and Processing
59 Center (DCPC), organized taking into account both the internet network problems and the big
60 amount of data produced by the interferometer.

61 Interferometric data are indeed complex numbers, organized in a matrix where each pixel contains
62 both phase and amplitude information of the backscattered signal (Bamler and Hartl, 1998;
63 Antonello et al., 2004); the radar employed produced a 1001x1001 complex matrix (corresponding
64 to ~7 megabytes) every 5 minutes. Therefore, there was the need to reduce the massive data flow
65 produced by the radar. For this reason data were locally and automatically elaborated in order to
66 produce, from a complex matrix, a simple ASCII grid containing only the pixel by pixel
67 displacement value, which is derived from the phase information. Then, since interferometry only
68 measures the displacement component projected along the radar line of sight, data needed to be re-
69 projected. This was performed by dividing the ASCII grid by a correction matrix, where every
70 element of the matrix was the percentage of the actual displacement that was measurable by the
71 radar; such percentage can be obtained with trigonometrical arguments knowing the position of the
72 radar and the direction of movement of the landslides (which, in our case, corresponded with the
73 slope direction) thus enabling the calculation of the radar line of sight.

74 To further reduce the size of the grids, matrixes where cropped in order to contain only those pixels
75 where relevant information could be extracted.

76 The ASCII grids where also averaged to reduce noise, so 8-hours and 24-hours averaged grids were
77 obtained. According to the early warning procedures that were defined, during periods characterized
78 by low or null slope movement, only 8-hours and 24-hours data where transferred, together with the
79 last displacement measurement of a reduced number of control points.

80 The transfer was performed after transforming the grids into strings and by sending them through a
81 middleware to the Data Acquisition and Elaboration Centre, where control points displacement



82 values where compared with warning thresholds and the grids where projected on a GIS
83 environment as 2D displacement maps.

84 **3 Materials and methods**

85 *3.1 GB-InSAR*

86 The ground-based interferometric synthetic aperture radar (GB-InSAR) is composed of a
87 microwave transceiver mounted on a linear rail (Tarchi et al., 1997; Rudolf et al., 1999; Tarchi et
88 al., 1999). The system used is based on a Continuous Wave – Stepped Frequency radar, which
89 moves along the rail at millimeter steps, in order to perform the synthetic aperture; the longer the
90 rail the higher the cross-range resolution. The microwave transmitter produces, step-by-step,
91 continuous waves around a central frequency, which influences the cross-range resolution and
92 determines the interferometric sensitivity i.e. the minimum measurable displacement, usually
93 largely smaller than the corresponding wavelength.

94 The radar produces complex radar images containing the information relative to both phase and
95 amplitude of the microwave signal backscattered by the target. The amplitude of a single image
96 provides the radar reflectivity of the scenario at a given time, while the phase of a single image is
97 not usable. The technique that enables to retrieve displacement information is called interferometry
98 and requires the phase from two images. In this way it is possible to elaborate a displacement map
99 relative to the elapsed time between the two acquisitions.

100 The main added value of GB-InSAR is its capability of blending the boundary between mapping
101 and monitoring, by computing 2D displacement maps in near real-time. The use of this tool to
102 monitor structures, landslides, volcanoes, sinkholes is largely documented (Calvari et al., 2016; Di
103 Traglia 2014; Intrieri et al., 2015; Bardi et al., 2016, 2017; Martino and Mazzanti, 2014; Severin,
104 2014; Tapete et al., 2013), as well as for early warning and forecasting (Intrieri et al., 2012; Carlà et
105 al., 2016a; 2016b; Lombardi et al., 2016).

106 GB-InSAR systems probably reveal their full potential in emergency conditions. They are
107 transportable and only require from few tens of minutes to few hours to be installed (depending on
108 the logistics of the site). Moreover, they are able to detect "near-real time" area displacements,
109 without accessing the unstable area, 24h and in all weather conditions (Del Ventisette et al., 2011;
110 Luzi, 2010; Monserrat et al., 2014). On the other hand, some limitations reduce the GB-InSAR
111 technique applicability: first of all the scenario must present specific characteristics in order to
112 reflect microwave radiations, maintaining high coherence values (Luzi, 2010; Monserrat et al.,
113 2014); only a component of the real displacement vector can be identified (i.e. the component
114 parallel to the sensor's line of sight); maximum detectable velocities are connected to the time that
115 the system needs to obtain two subsequent acquisitions. Sensors need power supply that, for long
116 term monitoring, cannot be replaced by batteries, generators or solar panels.

117 With the specific aim of performing an early warning system, data acquired *in situ* must be sent
118 automatically to a "control center" where they are integrated in a complete early warning system
119 procedure (Intrieri et al., 2013). In this sense, another main limitation is represented by the necessity
120 to transfer a high quantity of data, whose weight has to be reduced to the minimum, in order to
121 reduce the load on transmission network.



122 The employed system is a portable device designed and implemented by the Joint Research Center
123 (JRC) of the European Commission and its spin-off company Ellegi-LiSALab (Tarchi et al., 2003;
124 Antonello et al., 2004). The linear rail is 210 cm long, allowing a synthetic aperture of maximum
125 180 cm. It is easily transported by a normal motorized vehicle but its length is enough to obtain
126 high cross-resolution images, also at a distance from the scenario the can reach more than 1 km.
127 The transmitter and receiver move on the rail on a specific support, which can be tilted in order to
128 direct the microwave radiation as much as possible parallel to the displacement direction. The
129 power base represents the control center of the system; it contains a personal computer that
130 manages the definition of input parameters used in the acquisition phase and a UPS (Uninterruptible
131 Power Supply) to guarantee constant electric supply; it also enables data elaboration and storage,
132 being equipped with two boards increasing the memory to 1.8 TiB. The employed system needs 850
133 W, 230 VAC and 50 Hz as power supply. The integrated UPS guarantees the continuity of the
134 electric supply in case of necessity, for a period of maximum 12 hours after the power cut. The total
135 weight of the instrument is 95 kg, equally distributed over the different components (power base
136 with UPS and boards, transceiver, linear rail).

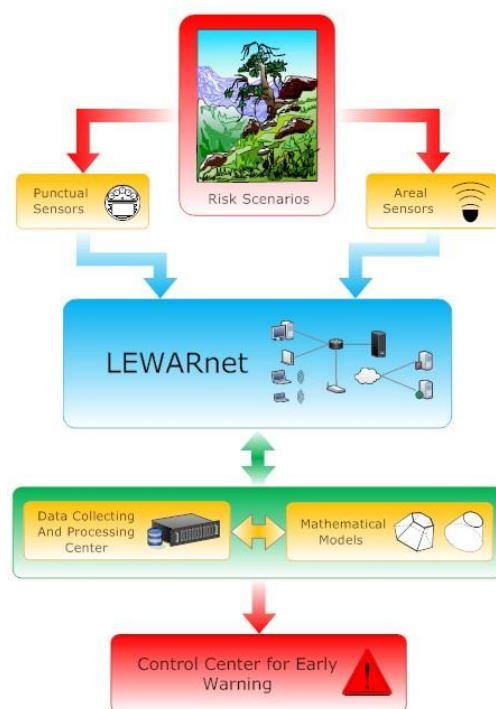
137 *3.2 Early warning system architecture*

138 Morphological features, hydrogeological factors and sudden rainfall can cause different types of
139 movements or fall of earthy and rock materials. The unpredictability and diversity of these events
140 make structural interventions often inappropriate to reduce the related risk, and real time monitoring
141 network difficult to implement.

142 In the last decade, Wireless Sensor Networks (WSNs) have been largely used in various fields. A
143 significant increase in the use of WSN, due to their simplicity, low cost of installation,
144 manufacturing and maintenance, has been recorded in the framework of environmental monitoring
145 applications (Intrieri et al., 2012; Liu et al., 2007; Yoo et al., 2007). Different types of sensor nodes
146 of these networks, distributed with high density in the monitored areas, send environmental
147 information to the concentrators nodes, generating a considerable amount and a wide variety of
148 collected data. Due to the significant growth of data volumes to be transferred, the WSN require
149 flexible ad-hoc protocols, able to respect constraints related to energy consumption management
150 (Hadadian and Kavian, 2016; Khaday et al., 2015; Parthasarathy et al., 2015). In particular, many
151 protocols have been developed that offer data aggregation patterns to optimize the sensor nodes
152 battery life (Kim et al., 2015) or sleep/measurement/data transfer cycles to minimize the energy
153 consumption (Fei et al., 2013; Venkateswaran and Kennedy, 2013).

154 LEWIS (Costanzo et al., 2016) uses heterogeneous sensors, distributed in the risk areas, to monitor
155 the several physical quantities related to landslides. The measured data, through a
156 telecommunications network, flow into the Data Collecting And Processing Center (DCPC), where,
157 using suitable mathematical models for the monitored site, the risk is evaluated and eventually the
158 state of alert for mitigation action is released (Figure 1).

159 The system, through a modular architecture exploiting a telecommunication network (called
160 LEWARnet) based on an ad-hoc communication protocol and an adaptive middleware, has a high
161 flexibility, which allows for the use of different interchangeable technological solutions to monitor
162 the parameters of interest.



163

164

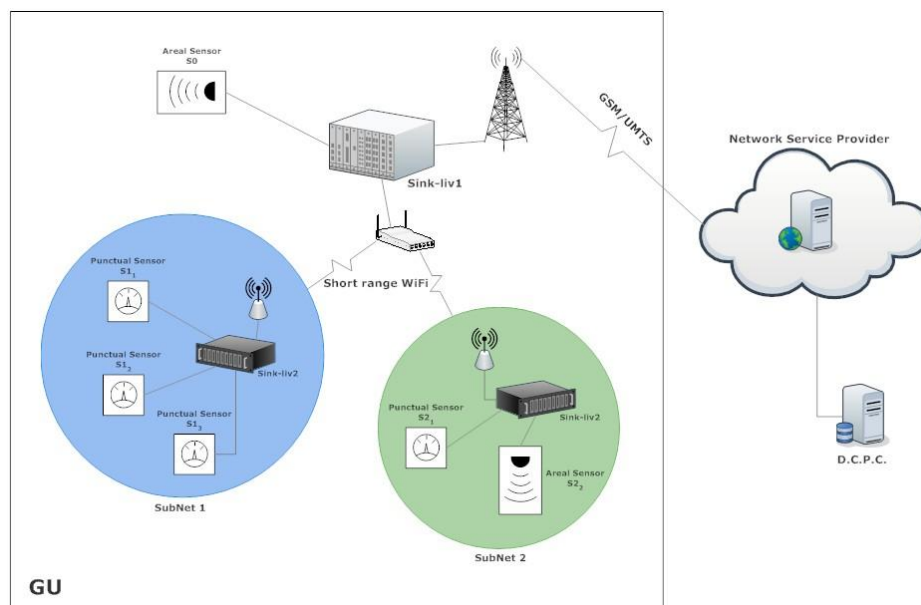
Figure 1. LEWIS architecture.

165 The telecommunication network has been designed and implemented within the Microwave
166 Laboratory of the University of Calabria.

167 The areas to be monitored have been divided into geomorphological units, indicated as GU. Each
168 GU is then subdivided into more heterogeneous sensors subnets.

169 For this purpose, each GU contains a concentrator node, called first level Sink, which has the
170 purpose of coordinating the sensors or any sub-network of sensors and collect the measurements
171 from them to transmit the data to the DCPC. Each sub-network is coordinated by a second level
172 Sink node, connected to the first level Sink through a short-range wireless connection (eg. ZigBee,
173 Bluetooth).

174 The network architecture can be schematized as shown in Figure 2.



175
176

Figure 2. LEWARnet architecture.

177 The network has been equipped with both single point sensors as well as area sensors, and the sub-
178 networks may include the use of a single type of these or both. The present paper addresses a sub-
179 network comprising an area sensor, the GB-InSAR.

180 The different sensors types generate asynchronous traffic, thus imposing the adoption of an ad-hoc
181 transmission protocol. This can support an asynchronous transmission mode to the DCPC, and it is
182 equipped with message queues management capacity to reconstruct historical data series, between
183 two connection sessions, in case of null or partial transmission. This operation mode requires the
184 presence of a software architecture that operates as a buffer, acting as an intermediary or as
185 middleware (LEWARnet), between the data consumer (DCPC) and the data producers (sensors and
186 sub-networks of sensors).

187 The developed middleware also monitors the processes of transmission and data acquisition,
188 recognizing the activity status of the sensors and that of the DCPC, and integrating encryption and
189 data compression functions.

190

191 *3.3 Data Collecting and Processing Center (DCPC)*

192 The management of information flows, the telematic architecture and the services for data
193 management are entrusted to the DCPC.

194 The DCPC has been designed and performed according to a complex hardware and software
195 system, able to ensure the reliability and continuity of the service, providing advance information of
196 possible dangerous situations that may occur.



197 In the research project, the DCPC has to ensure the continuous exchange of information among
198 monitoring networks, mathematical models and the Command and Control Center (CCC), that is
199 responsible for emergency management and decision making.

200 The design and implementation of procedures for the exchange of information from the monitored
201 sites to the CCC was built according to persistent and stable communication protocols, that are
202 suitable for hardware/software architecture of monitoring devices, for models and for CCC.

203 Data flow from the monitoring network was managed according to a communication protocol,
204 implemented by the DCPC, and named AqSERV. AqSERV was designed considering the
205 heterogeneity of devices of monitoring and transmission networks (single point and area sensors)
206 and the available hardware resources (microcontrollers and/or industrial computers). AqSERV was
207 devised to link DCPC database (named LEWISDB) to the monitoring networks, after validation for
208 the authenticity of the node that connects to the center. Data acquisition, before the storage in the
209 database, is validated both syntactically and according to the information content. The procedures
210 for extraction of the information content and validation have been realized differently for single
211 point and area sensors: the latter require a more complex validation, as they work in a 2D domain.

212 The complete management of the monitoring networks by DCPC has been realized through specific
213 remote commands, sent to individual devices via AqSERV, to reconfigure the acquisition intervals
214 or to activate any sensor, depending on the natural phenomena occurring in real time.

215 The acquired and validated data are then accessible for the mathematical models through a further
216 service, created ad hoc, which publishes all the acquisitions by sensors on a remote server for
217 sharing.

218 The configuration of monitoring networks, composed by devices and sensors, of communication
219 protocol used by each network, and of rules for extraction and validation of information content is
220 carried out through a web application that allows for the management of the whole system by the
221 users.

222 Besides the configuration, the application has been configured to automatically create the tables of
223 interest; automation of the process permits to reduce the acquisition time and possible human errors.

224 The real-time search for acquisitions is carried out through a WebGIS, specifically designed for
225 WSNs, but that can be easily extended to classic monitoring networks.

226 The WebGIS was designed according to the traditional web architecture, client-server, by using
227 network services which are web mapping oriented:

- 228 - web server for static data;
- 229 - web server for dynamic data;
- 230 - server for maps;
- 231 - database for the management of map data.

232 The static layers provided by the WebGIS are the results produced by geological studies for the
233 identification of event scenarios: geological map, geomorphological map, map of event scenarios.

234 The dynamic layers are the acquisitions in real time by the sensors.

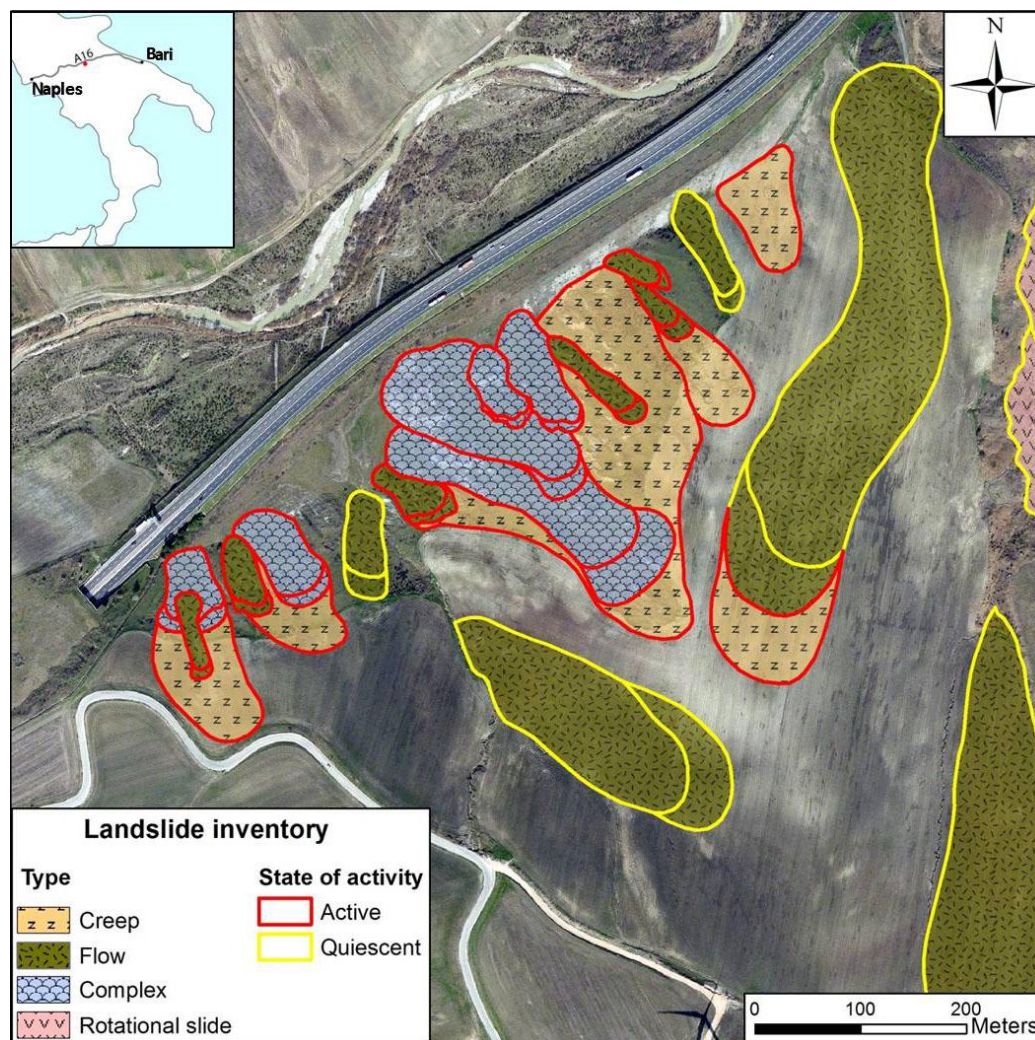
235 A DCPC operator can consult the information provided by each layer via a standard web browser
236 verifying the performance of the event precursors and any anomalies in acquisitions.

237 **4 Test site**

238 The test site chosen to experiment the integrated system is located in Southern Italy, along a section
239 of the A16 highway, an important communication route that connects Naples to Bari (Figure 3).



240 The A16 selected section develops in SW-NE direction, along the Southern Italian Apennine, in
241 correspondence with the valley of the Calaggio Creek, between the towns of Lacedonia (Campania
242 Region) and Candela (Puglia Region).



243
244 **Figure 3. Landslides detected through field survey along the monitored section of A16 highway.**

245 The area is tectonically active, but the landscape, characterized by gentle slopes, is mostly
246 influenced by lithologic factors (the strong presence of clayey sediments) rather than by tectonics.

247 The highway runs on the right flank of the Calaggio Creek at an altitude between 300 and 400 m
248 a.s.l.; the section of interest represents an element at risk in the computation of landslide risk
249 assessment, due to the presence of unstable areas which can potentially affect the communication
250 route (Figure 3). These unstable areas mainly involve clayey superficial layers.



251 On 1st July 2014, the GB-InSAR system has been installed on the test site. The location of the
252 installation point has been selected taking into account the view of the unstable area and the
253 distance from the power supply network. A covered structure was built in order to protect the
254 system from atmospheric agents and possible acts of vandalism, in the perspective of a long term
255 monitoring (Figure 4).



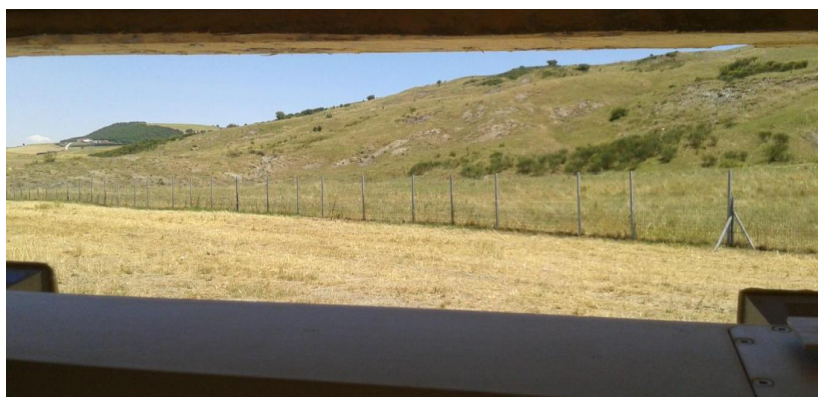
256

257 **Figure 4. Pictures of the construction of the covered structure and installation of the GB-InSAR.**

258 The transmission network was provided by a GSM modem, exploiting the 3G network. In addition
259 to the PC integrated in the GB-InSAR power base, a further external PC was exclusively employed
260 for data post elaboration and transmission.

261 The system acquired from the beginning of July 2014 until the end of July 2015.

262 The installation location allowed the system to detect an area between 40 and 400 meters far from
263 the its position in range direction, and about 360 m wide in the azimuth direction. These values,
264 coupled with a 40° vertical aperture of the antennas, allowed operators to detect an area of about
265 360 m x 360 m (Figure 5).



266

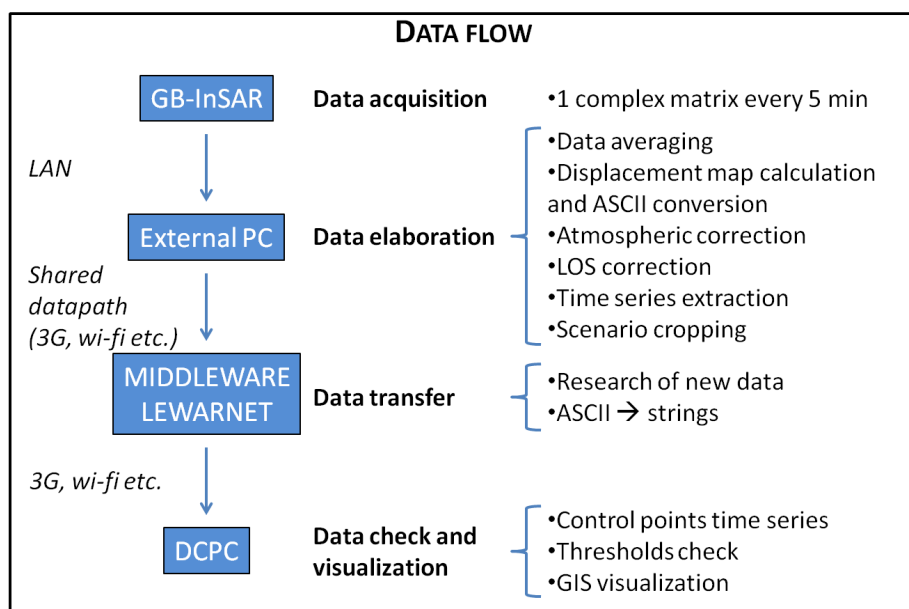


267

Figure 5. Field of view of the slope from the GB-InSAR installation point.

268 **5 Data management**

269 The most relevant matter of this monitoring was not as much related to the detection of landslide
 270 movements threatening the highway, as to how a long term monitoring performed with an
 271 instrument providing huge amounts of data could have been run without resorting to large hard
 272 drives nor to fast internet connections. For this reason an appropriate data management (Figure 6)
 273 was developed.



274

Figure 6. Diagram showing the complete data flow from acquisition to final visualization.

275

276 *5.1 Data acquisition*

277 The GB-InSAR employed produced a single radar image, consisting in a 1001x1001 complex
 278 matrix, every 5 minutes. Each one is around 8 Megabytes large, resulting in more than 2 Gigabytes
 279 of data produced every day.

280 This amount of data represented an issue for both store capacity and data transmission.

281 *5.2 Data elaboration*

282 After being acquired, data were then transferred through LAN connection to the external PC
 283 implementing a dedicated Matlab script locally performing the actions described as follows.



284 5.2.1 Data averaging

285 In order to reduce the noise normally affecting radar data (especially in vegetated areas), the images
286 acquired every 5 minutes were also averaged using all data of the previous 8 and 24 hours. Then
287 images averaged on 24 hours have been used to calculate daily displacement maps, every 8 hours to
288 create 8h displacement maps and non-averaged images to calculate 5 minutes displacement maps.
289 These time frames have been selected based on the characteristics of the slope movements and
290 signal/noise ratio in the investigated area.

291 Averaging is also a mean to make a good use of a high data frequency, since it enables to reduce the
292 memory occupied in the database as an alternative to their direct elimination.

293 5.2.2 Displacement map calculation and ASCII conversion

294 Each radar image can be represented as in Eq.1:

$$295 \quad S_n = A_n \exp(j\varphi_n) \quad (1)$$

296 where A_n is the amplitude of the n^{th} image, φ_n its phase and $j = (-1)^{1/2}$ is the imaginary unit. The
297 displacement Δr occurred in the time period between the acquisition of S_1 and S_2 has been
298 calculated with the following (Eq.2):

$$299 \quad \Delta r = (\lambda/4\pi) \cdot \Delta\varphi \quad (2)$$

300 where λ is the wavelength of the signal and

$$301 \quad \Delta\varphi = \varphi_1 - \varphi_2 \quad (3)$$

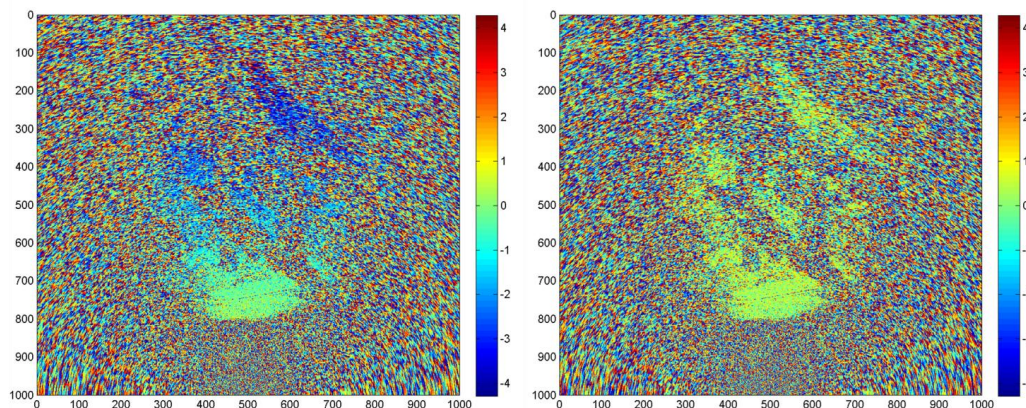
302 can be derived from:

$$303 \quad S_3 = S_1 S_2^* = A_1 A_2 \exp[j(\varphi_1 - \varphi_2)] \quad (4)$$

304 As a result, an ASCII file, only containing the information relative to the displacement for each
305 pixel, was obtained.

306 5.2.3 Atmospheric correction

307 One of the major advantages of GB-InSAR is the capability to achieve sub-millimeter precision.
308 However this can be severely hampered by the variations of air temperature and humidity,
309 especially when long distances are involved. Usually, atmospheric correction is performed by
310 choosing one area considered stable, taking into account that every displacement value different
311 from 0 is due to atmospheric noise and assuming that this offset is a linear function of the distance.
312 Based on this relation all the displacement map is corrected. In our case the whole scenario has been
313 selected and then only the potential unstable zones and those with a weak or incoherent
314 backscattered signal were removed. The remaining areas were then considered stable and therefore
315 were used for calculating the atmospheric effects. This results in a larger correction region that
316 enables a statistical correlation between the atmospheric effects and the distance and therefore the
317 calculation of a site-specific regression function that may not necessarily be linear (Figure 7).



318
 319 **Figure 7. The color bar is expressed in mm; green indicates stable pixels, while blue and red**
 320 **respectively movement toward and away from the GB-InSAR. Left: raw interferogram showing**
 321 **artificial displacement increasing linearly with distance (as typical of atmospheric noise). Right: the**
 322 **same interferogram after the atmospheric correction.**

323 5.2.4 Line of sight correction

324 The availability to detect only the LOS (Line Of Sight) component of the displacement vector
 325 represents one of the main limitations of the GB-InSAR technique. A method to partially overcome
 326 this limitation has been applied in this paper, following the procedure described in Colesanti &
 327 Wasowski, 2006 and later in Bardi et al. 2014 and 2016.

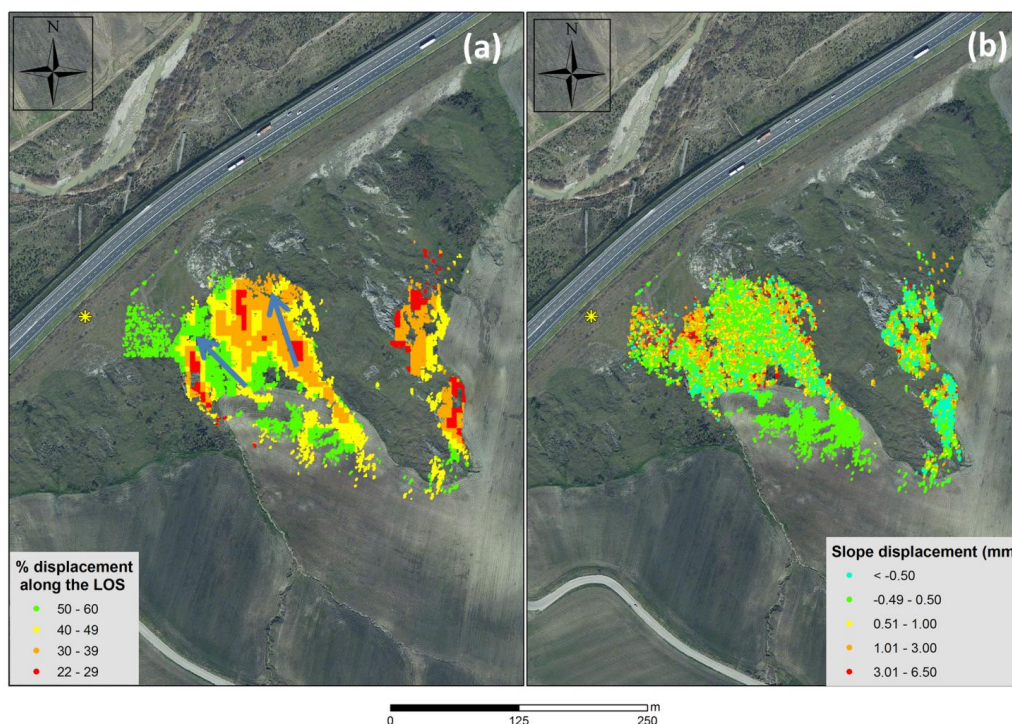
328 Assuming the downslope direction as the most probable displacement path, radar data have been
 329 projected on this direction. Input data as the angular values of *Aspect* and *Slope* have been derived
 330 from the *Digital Terrain Model* (DTM) of the investigated area; furthermore, azimuth angle and
 331 incidence angle of the radar LOS have been obtained.

332 After calculating the direction cosines of LOS and Slope (respectively functions of azimuth and
 333 incidence angles and aspect and slope angles) in the directions of Zenith (Z_{los} , Z_{slope}), North (N_{los} ,
 334 N_{slope}) and East (E_{los} , E_{slope}), the coefficient C is defined as follow (Eq. 5):

$$335 \quad C = Z_{los} \times Z_{slope} + N_{los} \times N_{slope} + E_{los} \times E_{slope} \quad (5)$$

336 C represents the percentage of real displacement detected by the radar sensor (Figure 8A).

337 The real displacement (D_{real}) is defined as the ratio between the displacement recorded along the
 338 LOS (D_{los}) and the C value (Figure 8 B).



339

340 **Figure 8. (a) *C* values map. Blue arrows indicate the downslope direction. (b) Cumulated displacement**
341 **values projected along the downslope direction, referred to a period between 1 July 2014 and 1**
342 **November 2014.**

343 Assuming that the studied landslide actually moves along the downslope direction, the GB-InSAR
344 detectable real displacement percentage ranges between 22 and 60 % (Figure 8A).

345 In Figure 8B, an example of slope displacement map has been shown. Here, cumulated
346 displacement data related to a period between 1 July and 1 November 2014 have been projected
347 along the downslope direction. Data show as the area can be considered stable in the referred
348 period; maximum displacement values of 4 mm in 4 months (eastern portion of observed scenario)
349 can be still considered in the range of stability.

350 5.2.5 Time series extraction

351 In order to allow for a fast data transfer and velocity threshold comparison, some representative
352 control points were selected, aimed at providing cumulated displacement time series. Control points
353 were retrieved from the same displacement maps calculated as described in paragraph 5.2.2 and
354 therefore can be relative to a time frame of 5 minutes, 8 hours or 24 hours.

355 In case of noisy data, instead of having a time series relative to a single pixel, these can be retrieved
356 from a spatial average obtained from a small area consisting of few pixels.



357 5.2.6 Scenario cropping

358 Typically, the field of view of a GB-InSAR is larger than the actual area to be monitored. In fact, a
359 portion of the radar image may be relative to the ground, sky, areas geometrically shadowed or
360 covered by dense vegetation. These may be of no interest or even containing no information at all.
361 For the case here studied around 50% of a radar image had a low coherence and was for all practical
362 purposes, unusable. Therefore, a cropping of the ASCII displacement map occurred in order to
363 frame only the relevant area.

364 5.3 Data transfer and visualization

365 The interferometric data generated by GB-InSAR, after the pre-processing and proper correction
366 previously described, are ready for transfer to the DCPC. The transmission of these data to the
367 DCPC is mediated by the middleware, which interrogates the GB-InSAR for tracking the state,
368 detects the newest data, and reorders and marks them to properly build data time series to be
369 transferred to DCPC.

370 Subsequently, the middleware manages communications with the DCPC, according to the
371 implemented ad-hoc protocol. This ensures the security of data providers through encrypted
372 authentication mechanisms, it allows for recovering missing or partially transmitted data, thus
373 avoiding information loss, and provides data acquired by the sensors to the DCPC in a standardized
374 format, JSON, able to guarantee uniformity between the various information provided by the
375 various sensors types. All these particular features fully justify the adoption of an ad-hoc protocol
376 for data transfer, instead of using a standard protocol such as FTP.

377 The data files produced by the GB-InSAR have already been locally pre-processed and result in a
378 matrix expressed in ASCII code; the dimensions of the matrix are known and range from 1x1 (for
379 the displacement of single control points) to 1001x1001 (for uncropped displacement maps). Before
380 encapsulating these data in the message to be transferred to DCPC, the middleware converts them
381 from ASCII code to character strings, using the standard coding ISO / IEC 8859-1, so being able to
382 obtain a data compression with a factor equal to ≈ 8 .

383 Eventually the DCPC is entrusted for cumulating the displacements relative to the control points,
384 which are compared with the respective thresholds, and for visualizing the displacement maps as
385 WebGIS layers, thus enabling data validation and the evaluation of the extension of moving surface.

386 **6 Early warning procedures discussions**

387 The GB-InSAR is part of a larger early warning system (LEWIS) which also includes other
388 monitoring systems and simulation models. Therefore, to understand how GB-InSAR data can be
389 used in an early warning perspective, it is necessary to make reference to LEWIS as a whole.

390 Any information, coming from the investigated sites and subsequently processed also by using the
391 simulation models, is used to define an intervention model. This is based on the following elements:
392 event scenarios, risk scenarios, levels of criticality, levels of alert.

393 Event scenarios describe the properties of expected phenomena in terms of dimension, velocity,
394 involved material and occurrence probability. Occurrence probability depends on the associated
395 time horizon, which should be equal to few hours at most, in the case of early warning systems.



396 Evaluation of occurrence probability is carried out by using information from monitoring systems
397 and/or from outputs of adopted mathematical models for nowcasting. All the properties, to be
398 analyzed for event scenarios, are listed below; a subdivision in classes is adopted for each one:

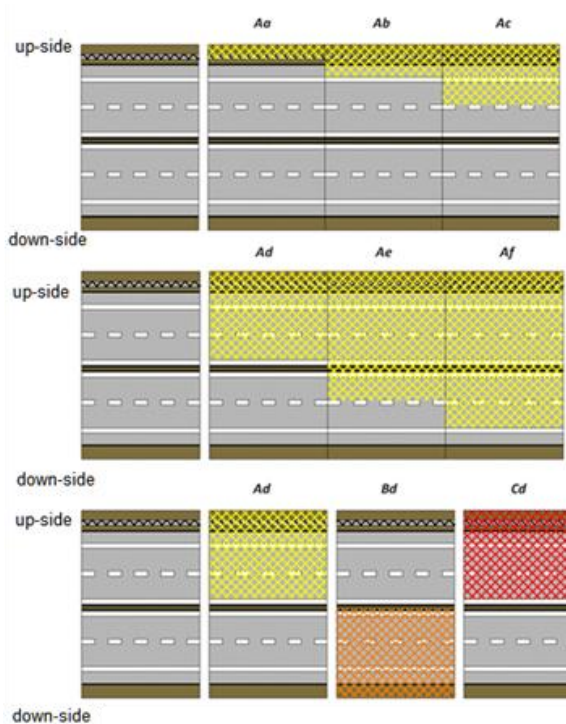
- 399 • landslide velocity (5 classes from slow to extremely rapid);
- 400 • landslide surface (5 classes from very small to very large);
- 401 • landslide scarp (5 classes from very small to very large);
- 402 • landslide volume (5 classes from extremely small to large);
- 403 • thickness (5 classes from very shallow to very deep);
- 404 • magnitude (3 classes: low, moderate, high), which combines the previous information;
- 405 • involved material (mud, debris, earth, rock, mixture of components);
- 406 • occurrence probability (zero, low, moderate, high, very high, equal to 1).

407 While some of the aforementioned parameters are determined by geological surveys, landslide
408 velocity is directly derived from monitoring data (such as those collected by GB-InSAR). Landslide
409 surface can be determined by geomorphological observation but is precisely quantified by GB-
410 InSAR, thanks to its capability of producing 2D displacement maps.

411 Risk scenarios can be firstly grouped in the following three classes:

- 412 A. mud and/or debris movements which could induce a friction reduction and facilitate slips;
- 413 B. road subsidence induced by landslides that could drag or drop vehicles;
- 414 C. falls of significant volumes and/or boulders that could crush or cover vehicles and constitute
415 an obstacle for others vehicles.

416 For each previous risk scenario, six sub-scenarios can be identified on the basis of the number of
417 potentially involved infrastructures, carriageways and lanes (a. hydraulic infrastructures and/or
418 barriers, b. only emergency lane, c. lane, d. fast lane, e. fast lane of the opposite carriageway, f. lane
419 of the opposite carriageway). Thus, all possible risk scenarios are 18 (Figure 9) , indicated with a
420 couple of letters (Capital and small).



421
 422 **Figure 9. Top and middle: possible risk scenarios involving the scenario A (landslides that could**
 423 **reduce friction) to increasing sectors of the highway. Bottom: combinations of scenarios with different**
 424 **types of phenomena (A, B, C) affect the emergency lane, lane and fast lane.**

425 The following information is provided to DCPC:

- 426 • Measurements from sensors
- 427 • Model outputs

428 and four states are identified for each of them:

- 429 • state 0 = no variation
- 430 • state 1 = small variation
- 431 • state 2 = moderate variation
- 432 • state 3 = high variation.

433 Besides information from sensors and models, other information is obtained from meteorological
 434 and hydrological models (named as indicators).

435 Indicators comprise weather forecasting and output of FLAIR and Sushi models (Sirangelo et al.
 436 2003; Capparelli and Versace 2011) on the basis of observed and predicted (for the successive six
 437 hours) rainfall heights.

438 Two states are defined for indicators:

- 439 • state 0 = no variation or not significant,
- 440 • state 1 = significant variation.

441 To sum up, DCPC has the following information in any moment:

- 442 ▶ state (0, 1) of indicators (IND),
- 443 ▶ state (0, 1, 2, 3) of sensors and models running for the specific highway section (SEN),



444 and, on the basis of these states, four different decisions can be made by DCPC, one of which with
 445 three options.
 446 All the possible decisions are illustrated in Table 1, in which the weight of the several sensors is
 447 assumed to be the same. Based on the notices of criticality levels provided by the DCPC, and on its
 448 own independent evaluations, the CCC issues the appropriate warning notices (Surveillance, Alert,
 449 Alarm and Warning) and makes decisions about the consequent actions.
 450

State of sensors and/or models	DCPC decisions
All INDs and SENs are S0	0 - no decision
At least one IND is S1 and all SENs are S0	1 – SOD (Sensor On Demand) activation
At least one SEN is S1	2 – to intensify the presence up to 24 hours/day
At least n SENs are S1 or at least one SEN is S2	3/1 – to issue a notice of ordinary criticality (level 1)
At least n SENs are S2 or at least one SEN is S3	3/2 - to issue a notice of moderate criticality (level 2)
At least n SENs are S3	3/3 - to issue a notice of high or severe criticality (level 3)

451

Table 1. DCPC possible decisions.

452 The information of each sensor and the results produced by the models are used to assess, in each
 453 instant, the occurrence probability of an event scenario in the monitored areas and the possible risk
 454 scenarios.

455 This combination of heterogeneous data was carried out by identifying for each sensor and model a
 456 typical information (displacement, precipitation, inclination, etc.), evaluating the state in each
 457 instant, according to a threshold system, and combining this result for all sensors placed in a
 458 monitored geomorphological area.

459 The final result is constituted by the occurrence probability of an event scenario, that is associated
 460 with a specific action by the DCPC. In particular, if the occurrence probability is low, moderate or
 461 high it is necessary to issue a notice of criticality (ordinary - Level 1, moderate - Level 2, High -
 462 Level 3) to the CCC.

463 The DCPC sends two types of information:

- 464 1) criticality state of the single monitored geomorphological unit,
- 465 2) criticality state of the whole area.

466 The adopted communication protocol between the two centers for the exchange of information was
 467 carried out through a web service provided by the CCC, using the classes and attributes of the
 468 methodology named Datex II (which is a protocol for the exchange of traffic data). The use of the
 469 web service allowed to ensure the interoperability of data between the two centers, regardless of the
 470 used hardware and software architecture, through a persistent service capable of ensuring an
 471 immediate restoration of the connections, in case of malfunction and a continuous monitoring
 472 between the two centers, even in the absence of criticality.

473



474 **7 Conclusions**

475 The GB-InSAR is a monitoring tool that is becoming more and more used in landslide monitoring
476 and early warning, especially thanks to its capability of producing real-time, 2D displacement maps.
477 On the other hand, it still suffers from some drawbacks, such as the limitation of measuring only the
478 LOS component of a target's movement and logistic issues like those owing to a massive
479 production of data that may cause trouble for both storing capacity and data transfer.

480 These problems have been addressed when a GB-InSAR was integrated within a complex early
481 warning system (LEWIS) and only a limited internet connection was available. This situation
482 required that a series of pre-elaboration processes and data management procedures took place in
483 situ, in order to produce standardized and reduced files, carrying only the information needed when
484 it was needed. The procedures mainly concerned the transmission of data averaged over determined
485 time frames, proportionate with the kinematics of the monitored phenomenon. Before, transmission
486 data were also corrected (both in terms of atmospheric noise and LOS) and reduced, by filtering out
487 the information relative to the amplitude of the targets, by eliminating the areas not relevant for the
488 monitoring and by transforming the matrices into strings.

489 As a result, GB-InSAR data converged into the early warning system and contributed to it by
490 producing displacement time series of representative control points to be compared with fixed
491 thresholds. Displacement maps were also available for data validation by expert operators and for
492 retrieving information relative to the surface of the moving areas.

493

494 *Competing interests.* The authors declare that they have no conflict of interest.

495

496 *Acknowledgements.* This research is part of the project "LEWIS (Landslides Early Warning
497 Integrated System): An Integrated System for Landslide Monitoring, Early Warning and Risk
498 Mitigation along Lifelines", financed by the Italian Ministry of Education, Universities and
499 Research and co-funded by the European Regional Development Fund, in the framework of the
500 National Operational Programme 2007-13 "Research and Competitiveness", grant agreement no.
501 PON01_01503.

502 The Authors are thankful to Giuseppe Della Porta and his colleagues from Autostrade S.p.A. for
503 their availability in permitting and supporting the installation and maintenance of the GB-InSAR
504 along the A16 highway.

505 **References**

506 Antonello, G., Casagli, N., Farina, P., Leva, D., Nico, G., Sieber, A. J., Tarchi, D.: Ground-based
507 SAR interferometry for monitoring mass movements. *Landslides*, 1 (1), 21-28, 2004

508 Baldrige, S.M., Marshall, J.D.: Performance of structures in the January 2010 MW 7.0 Haiti
509 earthquake. In: *Structures Congress*, 2011. doi: 10.1061/41171(401)145

510 Bamler, R. and Hartl, P.: Synthetic Aperture Radar Interferometry. *Inverse Problems*, 14, R1-R54,
511 1998.



- 512 Bardi, F., Frodella, W., Ciampalini, A., Del Ventisette, C., Gigli, G., Fanti, R., Basile, G., Moretti,
513 S., Casagli, N.: Integration between ground based and satellite SAR data in landslide mapping: The
514 San Fratello case study”, *Geomorphology*, 223, 45-60, 2014.
- 515 Bardi, F., Raspini, F., Ciampalini, A., Kristensen, L., Rouyet, L., Lauknes, T. R., Frauenfelder, R.
516 & Casagli, N.: Space-Borne and Ground-Based InSAR Data Integration: The Åknes Test Site.
517 *Remote Sensing*, 8(3), 237, 2016.
- 518 Bardi, F., Raspini, F., Frodella, W., Lombardi, L., Nocentini, M., Gigli, G., Morelli, S., Corsini, A.,
519 Casagli, N.: Monitoring the Rapid-Moving reactivation of Earth Flows by Means of GB-InSAR:
520 The April 2013 Capriglio Landslide (Northern Appennines, Italy). *Remote Sensing*, 9(2), 165, 2017.
- 521 Cagno, E., De Ambroggi, M., Grande, O., Trucco, T.: Risk analysis of underground infrastructures
522 in urban areas. *Reliability Engineering & System Safety* 96, 139-148, 2011.
- 523 Calvari, S., Intrieri, E., Di Traglia, F., Bonaccorso, A., Casagli, N., Cristaldi, A.: Monitoring crater-
524 wall collapse at active volcanoes: a study of the 12 January 2013 event at Stromboli. *Bulletin of*
525 *Volcanology*, 78 (5), 39, 2016.
- 526 Capparelli, G., Versace, P.: FLAIR and SUSHI: Two mathematical models for early warning of
527 landslides induced by rainfall. *Landslides*, 8 (1), 67-79, 2011.
- 528 Carlà, T., Intrieri, E., Di Traglia, F., Casagli, N.: A statistical-based approach for determining the
529 intensity of unrest phases at Stromboli volcano (Southern Italy) using one-step-ahead forecasts of
530 displacement time series. *Natural Hazards*, 84 (1), 669-683, 2016a.
- 531 Carlà, T., Intrieri, E., Di Traglia, F., Nolesini, T., Gigli, G., Casagli, N.: Guidelines on the use of
532 inverse velocity method as a tool for setting alarm thresholds and forecasting landslides and
533 structure collapses. *Landslides*, 14(2), 517-534, 2016b.
- 534 Colesanti, C. and Wasowski, J.: Investigating landslides with space-borne Synthetic Aperture Radar
535 (SAR) interferometry. *Eng. Geol.* , 88, 173–199, 2006.
- 536 Costanzo, S., Di Massa, G., Costanzo, A., Borgia, A., Raffo, A., Viggiani, G., Versace, P.:
537 Software-defined radar system for landslides monitoring. *Advances in Intelligent Systems and*
538 *Computing*, 445, pp. 325-331, 2016.
- 539 Del Ventisette, C., Intrieri, E., Luzi, G., Casagli, N., Fanti, R., Leva, D.: Using ground based radar
540 interferometry during emergency: The case of the A3 motorway (Calabria Region, Italy) threatened
541 by a landslide. *Natural Hazards and Earth System Science*, 11 (9), 2483-2495, 2011.
- 542 Di Traglia, F.; Nolesini, T.; Intrieri, E.; Mugnai, F.; Leva, D.; Rosi, M.; Casagli N.: Review of ten
543 years of volcano deformations recorded by the ground-based InSAR monitoring system at
544 Stromboli volcano: a tool to mitigate volcano flank dynamics and intense volcanic activity. *Earth*
545 *Science Reviews*, 139, 317-335, 2014.
- 546 Fei, X., Zheng, Q., Tang, T., Wang, Y., Wang, P., Liu, W., Yang H.: A reliable transfer protocol for
547 multi-parameter data collecting in wireless sensor networks”, 2013 15th International Conference on
548 Advanced Communication Technology: Smart Services with Internet of Things, ICACT 2013, 569-
549 573, 2013.



- 550 Geertsema, M., Schwab, J.W., Blais-Stevens, A., Sakals, M.E.: Landslides impacting linear
551 infrastructure in west central British Columbia. *Natural Hazards*, 48, 59-72, 2009.
- 552 Gene Corley, W., Mlakar, P.F.Sr., Sozen, M.A., Thornton, C.H.: The Oklahoma city bombing:
553 Summary and recommendations for multihazard mitigation. *J. Perform. Constr. Facil.* 12, 100-112,
554 1998.
- 555 Hadadian, H. and Kavian, Y.: Cross-layer protocol using contention mechanism for supporting big
556 data in wireless sensor network", 2016 10th International Symposium on Communication Systems,
557 Networks and Digital Signal Processing (CSNDSP), 2016.
- 558 Intrieri, E., Gigli, G., Mugnai, F., Fanti, R., Casagli, N.: Design and implementation of a landslide
559 early warning system. *Engineering Geology*, 147-148, 124-136, 2012.
- 560 Intrieri, E., Gigli, G., Casagli, N., Nadim, F.: Brief communication Landslide Early Warning
561 System: Toolbox and general concepts. *Natural Hazards and Earth System Science*, 13 (1), pp. 85-
562 90, 2013.
- 563 Intrieri, E., Gigli, G., Nocentini, M., Lombardi, L., Mugnai, F., Casagli, N.: Sinkhole monitoring
564 and early warning: An experimental and successful GB-InSAR application. *Geomorphology*, 241,
565 304-314, 2015.
- 566 Kadri, F., Birregah, B., Châtelet, E.: The impact of natural disasters on critical infrastructures: A
567 domino effect-based study. *Journal of Homeland Security and Emergency Management*, 11, 217-
568 241, 2014.
- 569 Khaday, B., Matson, E. T., Springer, J., Kwon, Y.K., Kim, H., Kim, S., Kenzhebalin, D., Sukyeong,
570 C., Yoon, J., Woo, H. S.: Wireless Sensor Network and Big Data in Cooperative Fire Security
571 system using HARMS, 2015 6th International Conference on Automation, Robotics and
572 Applications (ICARA), 2015.
- 573 Kim, Y., Bae, P., Han, J., Ko, Y.B.: Data aggregation in precision agriculture for low-power and
574 lossy networks", 2015 IEEE Pacific Rim Conference on Communications, Computers and Signal
575 Processing (PACRIM), 2015.
- 576 Kröger, W.: Critical infrastructures at risk: A need for a new conceptual approach and extended
577 analytical tool. *Reliability Engineering & System Safety*, 93, 1781-1787, 2008.
- 578 Labaka, L., Hernantes, J., Sarriegi, J.M.: A holistic framework for building critical infrastructure
579 resilience. *Technological Forecasting and Social Change*, 103, 21-33, 2016.
- 580 Liu, H., Meng, Z., Cui S.: A Wireless Sensor Network Prototype for Environmental Monitoring in
581 Greenhouses", 2007 International Conference on Wireless Communications, Networking and
582 Mobile Computing, 2007.
- 583 Lombardi, L., Nocentini, M., Frodella, W., Nolesini, T., Bardi, F., Intrieri, E., Carlà, T., Solari, L.,
584 Dotta, G., Ferrigno, F., Casagli, N.: The Calatabiano landslide (southern Italy): preliminary GB-
585 InSAR monitoring data and remote 3D mapping. *Landslides*, 1-12, 2016.
- 586 Luzi G.: Ground Based SAR Interferometry: a novel tool for geoscience. P. Imperatore, D. Riccio
587 (Eds.), *Geoscience and Remote Sensing. New Achievements, InTech*, 1-26, 2010. (Available at:



- 588 [http://www.intechopen.com/articles/show/title/ground-based-sar-interferometry-a-novel-tool-for-](http://www.intechopen.com/articles/show/title/ground-based-sar-interferometry-a-novel-tool-for-geoscience)
589 [geoscience](http://www.intechopen.com/articles/show/title/ground-based-sar-interferometry-a-novel-tool-for-geoscience)).
- 590 Martino, S., Mazzanti, P.: Integrating geomechanical surveys and remote sensing for sea cliff slope
591 stability analysis: The Mt. Pucci case study (Italy). *Natural Hazards and Earth System Sciences*, 14
592 (4), 831-848, 2014.
- 593 Monserrat, O., Crosetto, M., Luzi, G.: A review of ground-based SAR interferometry for
594 deformation measurement. *ISPRS J Photogramm*, 93, 40–48, 2014,
- 595 Parthasarathy, A., Chaturvedi, A., Kokane, S., Warty, C., Nema, S.: Transmission of big data over
596 MANETs. 2015 IEEE Aerospace Conference, 2015.
- 597 Rudolf, H., Leva, D., Tarchi, D., Sieber, A.J.: A mobile and versatile SAR system. 1999 IGARSS
598 Proc, Hamburh, 1999.
- 599 Severin, J., Eberhardt, E., Leoni, L., Fortin, S.: Development and application of a pseudo-3D pit
600 slope displacement map derived from ground-based radar. *Engineering Geology*, 181, 202-
601 211,2014.
- 602 Sirangelo, B., Versace, P., Capparelli, G.: Forewarning model for landslides triggered by rainfall
603 based on the analysis of historical data file. *IAHS-AISH Publication*, 278, 298-304, 2003.
- 604 Snyder, L., Burns, A.A.: Framework for critical infrastructure resilience analysis. *Energy and*
605 *systems analysis-infrastructure*. Sandia National Laboratories, 2009
- 606 Tapete, D., Casagli, N., Luzi, G., Fanti, R., Gigli, G., Leva D.: Integrating radar and laser-based
607 remote sensing techniques for monitoring structural deformation of archaeological monuments.
608 *Journal of Archaeological Science*, 40(1), 176-189, 2013.
- 609 Tarchi, D., Ohlmer, E., Sieber, A.J.: Monitoring of structural changes by radar interferometry. *Res.*
610 *Non Destr. Eval.*, 9, 213-225, 1997.
- 611 Tarchi, D., Rudolf, H., Luzi, G., Chiarantini, L., Coppo, P., Sieber, A. J.: SAR interferometry for
612 structural change detection: a demonstration test on a dam. *Proc. of Geoscience and Remote*
613 *Sensing Symposium, IGARSS 1999*, 3, 1525-1527, 1999.
- 614 Tarchi, D., Casagli, N., Fanti, R., Leva, D., Luzi, G., Pasuto, A., Pieraccini, M., Silvano, S.:
615 Landslide monitoring by using ground-based SAR interferometry: an example of application to the
616 Tessina landslide in Italy. *Engineering Geology*, 1, 68, 15-30, 2003.
- 617 Urlainis, A., Shohet, I.M., Levy, R., Ornai, D., Vilnay, O.: Damage in critical infrastructures due to
618 natural and man-made extreme Events – A critical review. *Procedia Engineering*, 85, 529-535,
619 2014.
- 620 Urlainis, A., Shohet, I.M., Levy, R.: Probabilistic Risk Assessment of Oil and Gas Infrastructures
621 for Seismic Extreme Events. *Procedia Engineering*, 123, 590-598, 2015.
- 622 Venkateswaran, V. and Kennedy, I.: How to sleep, control and transfer data in an energy
623 constrained wireless sensor network. 2013 51st Annual Allerton Conference on Communication,
624 Control, and Computing (Allerton), 2013.
- 625 Versace, P., Capparelli, G., Leone, S., Artese, G., Costanzo, S., Corsonello, P., Di Massa, G.,
626 Mendicino, G., Maletta, D., Muto, F., Senatore, A., Troncone, A., Conte, E., Galletta, D.: LEWIS



- 627 project: An integrated system of monitoring, early warning and mitigation of landslides risk.
628 Rendiconti Online Societa Geologica Italiana, 21(1), 586-587, 2012.
- 629 Yoo, S., Kim, J., Kim, T., Ahn, S., Sung, J., Kim, D.: A2S: Automated Agriculture System based
630 on WSN. 2007 IEEE International Symposium on Consumer Electronics, 2007.